

## Accepted Manuscript

The Lipidation Profile of Aquaporin-0 Correlates with The Acyl Composition of Phosphoethanolamine Lipids in Lens Membranes

Vian S. Ismail, Jackie A. Mosely, Antal Tapodi, Roy A. Quinlan, John M. Sanderson

PII: S0005-2736(16)30234-6  
DOI: doi: [10.1016/j.bbamem.2016.06.026](https://doi.org/10.1016/j.bbamem.2016.06.026)  
Reference: BBAMEM 82260

To appear in: *BBA - Biomembranes*

Received date: 26 May 2016  
Revised date: 24 June 2016  
Accepted date: 30 June 2016



Please cite this article as: Vian S. Ismail, Jackie A. Mosely, Antal Tapodi, Roy A. Quinlan, John M. Sanderson, The Lipidation Profile of Aquaporin-0 Correlates with The Acyl Composition of Phosphoethanolamine Lipids in Lens Membranes, *BBA - Biomembranes* (2016), doi: [10.1016/j.bbamem.2016.06.026](https://doi.org/10.1016/j.bbamem.2016.06.026)

This is a PDF file of an unedited manuscript that has been accepted for publication. As a service to our customers we are providing this early version of the manuscript. The manuscript will undergo copyediting, typesetting, and review of the resulting proof before it is published in its final form. Please note that during the production process errors may be discovered which could affect the content, and all legal disclaimers that apply to the journal pertain.

## The Lipidation Profile of Aquaporin-0 Correlates with The Acyl Composition of Phosphoethanolamine Lipids in Lens Membranes

Vian S. Ismail,<sup>a,d</sup> Jackie A. Mosely,<sup>a</sup> Antal Tapodi,<sup>c</sup> Roy A. Quinlan<sup>b,c</sup> and John M. Sanderson<sup>a,c</sup>

<sup>a</sup> Chemistry Department, Durham University, Durham, DH1 3LE, UK

<sup>b</sup> School of Biological Sciences, <sup>c</sup> Biophysical Sciences Institute, Durham University, Durham, DH1 3LE, UK

<sup>d</sup> Department of Biology, Faculty of Science, Soran University, Soran, Kurdistan Regional Government, Iraq

### Abstract

The lens fiber major intrinsic protein (otherwise known as aquaporin-0 (AQP0), MIP26 and MP26) has been examined by mass spectrometry (MS) in order to determine the speciation of acyl modifications to the side chains of lysine residues and the N-terminal amino group. The speciation of acyl modifications to the side chain of one specific, highly conserved lysine residue (K238) and the N-terminal amino group of human and bovine AQP0 revealed, in decreasing order of abundance, oleoyl, palmitoyl, stearoyl, eicosenoyl, dihomo- $\gamma$ -linolenoyl, palmitoleoyl and eicosadienoyl modifications. In the case of human AQP0, an arachidonoyl modification was also found at the N-terminus. The relative abundances of these modifications mirror the fatty acid composition of lens phosphatidylethanolamine lipids. This lipid class would be expected to be concentrated in the inner leaflet of the lens fiber membrane to which each of the potential AQP0 lipidation sites is proximal. Our data evidence a broad lipidation profile that is both species and site independent, suggesting a chemical-based ester aminolysis mechanism to explain such modifications.

### 1. Introduction

Membrane-associated peptides are known to undergo intrinsic lipidation reactions by acyl transfer from membrane lipids [1]. The benchmark peptide for this process is melittin, which is lipidated in synthetic liposomes on the N-terminal amino group and on the side chains of internal lysine and, less commonly, serine residues [2,3]. In the intrinsic lipidation reactions of melittin, little selectivity is found for the aminolysis reaction with the *sn*-1 and *sn*-2 glyceryl esters, and the acyl group distribution of the lipidated products reflects the fatty acyl composition of the liposomal membrane. In principle, membrane-embedded proteins should be susceptible to similar reactions *in situ*, but this is still an open question and the importance of non-enzymatic acylations is still being established [4]. Lipidation events that do not correspond to any of the known consensus sequences for enzyme-mediated modifications and exhibit an acyl group profile that reflects the lipid composition of the proximal membrane leaflet would be the first evidence for non-enzymatic lipidation. The eye lens contains some of the oldest proteins in the mammalian body and integral membrane proteins, such as AQP0, are excellent candidates to test this hypothesis. There are two known lipidation sites in AQP0 one at the N-terminus and the other at Lys-238 (Fig. S1-S3) [5–7]. Neither match consensus sequences for enzymatically mediated lipidation events. *In vitro* palmitoylation of AQP0 has been shown to be a post-translational, rather than a co-translational, event [8]. The longevity of lens proteins such as AQP0 in the plasma membrane of lens fiber cells [7], and the fact that all intracellular organelles are

removed during lens fiber cell differentiation [9], provides conditions under which modifications by acyl transfer from the membrane lipids will accrue [10]. In this paper we examine the lipidation profile of AQP0 from bovine and human lenses, with the specific objective of determining the acyl group diversity at these known lipidation sites.

## 2. Materials and Methods

**Materials.** Bovine eye lenses were obtained from Linden Burradon Food Supply (FSA Approval No. 2056) from calves of age 6–12 months. Human lenses (22 years old) were obtained from the Bristol Eye Bank with national research ethics committee approval and were used as recommended by the Declaration of Helsinki and following the procedures recommended under the Human Tissue Authority license to the University of Durham. Proteomics grade trypsin from porcine pancreas was used (Sigma-Aldrich, Dorset, UK).

**Lens Membrane Extraction.** A sequential extraction procedure designed for integral membrane proteins [11] and adapted to purify lens membranes highly enriched in AQP0 [5,12] was used. Lenses were decapsulated and aqua-dissected by stirring in a buffer composed of 10 mM sodium phosphate (pH 7.4), 100 mM NaCl and 5 mM EDTA (buffer 1) to remove sequentially the youngest (cortical) fiber cells through to the oldest (nuclear) fiber cells. Cells were centrifuged and resuspended successively in buffers containing high salt, ammonium bicarbonate, urea and sodium hydroxide. At the conclusion of the extraction procedure, membrane pellets were stored in buffer 1 containing 0.02% sodium azide (w/v) as a preservative and kept at 4 °C until analysis.

**Intact Protein Analysis.** Bovine AQP0 was solubilized in buffer 1 by the addition of 0.8% perfluorooctanoic acid (w/v) before centrifugation (mini centrifuge, 1 min). The supernatant was analyzed by reverse phase LC using an Xbridge BEH300 C4 column (3.5 µm particle size, 2.1 mm internal diameter, 150 mm length, Waters Ltd., USA) with a flow rate of 200 µl/min and a linear gradient (A:B) of 95:5 to 5:95 over 10 min, then 0:100 for 5 min, where A is water and B is MeCN, both containing 0.1% formic acid (FA). An LC-FT-ICR mass spectrometer equipped with a 7 T magnet (LTQFT from ThermoFisher) was used to acquire positive ion mass spectra. Spectra were deconvolved using the Qual Browser software (ThermoFinnigan) and an overlapping time window approach.

**Trypsin Digestion.** An aliquot of 100 µl of resuspended AQP0 in buffer 1 plus 0.02% sodium azide was combined with 10 µl each of DTT (100 mM) and trypsin (0.2 mg/ml in 50 mM acetic acid) and incubated at 37 °C for 24 h. All AQP-0 digests were analyzed using an Xbridge C18 column (3.5 µm particle size, 2.1 mm internal diameter, 100 mm length, Waters UK). LC-FT-ICR analyses of b-AQP0 used the conditions described for intact protein analysis. LC-QToF MS (MS/MS and MS<sup>E</sup>) data were acquired on a Synapt G2-S (Waters) instrument, with time-of-flight (ToF) analyser. These separations used an Acuity UPLC<sup>TM</sup> system at a flow rate of 400 µl/min, gradient (A:B): 95:5 to 5:95 over 8 min. Tandem MS was performed by collision induced dissociation in the trap region of the triwave. MS/MS of an isolated precursor ion or MS<sup>E</sup> for the all ions were acquired with a trap collision energy ramp of 30–50 eV.

### 3. Results

#### Analysis of the Intact Protein

Intact bovine AQP0 (b-AQP0) was isolated from the outer part (cortex) of the lens by decapsulation followed by aqua-dissection. This section of the lens was selected to minimize potential complications that could arise from the presence of truncated protein; the extent of protein truncation increases in older fractions towards the nucleus of the lens [5,13]. The intact protein was analyzed by ESI-FT-ICR MS, yielding a spectrum (Fig. 1) containing several isotopomer envelopes, from which a number of b-AQP0 modifications can be discerned.

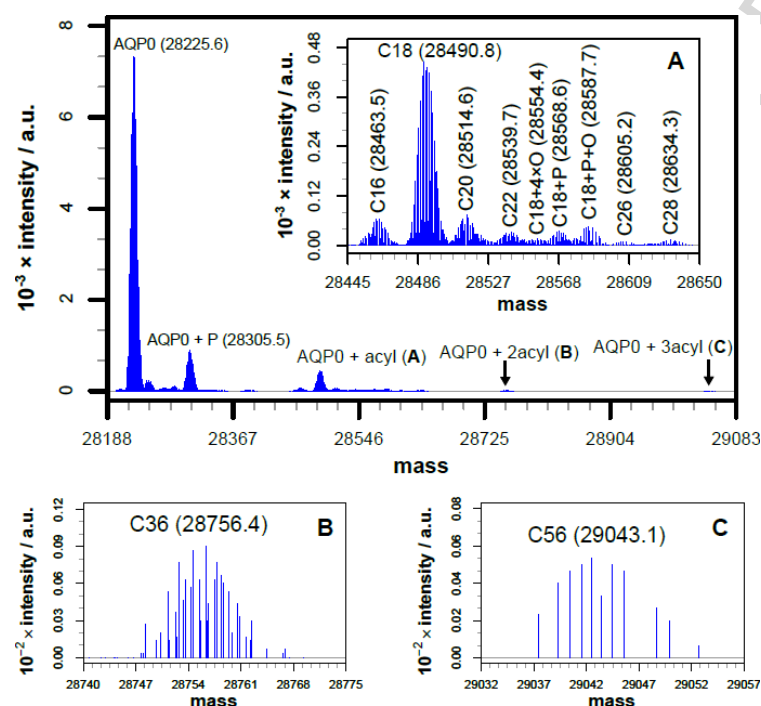


**Figure 1** - Charge state deconvoluted spectrum (neutral mass) of b-AQP0 from the outer lens cortex. The spectrum was obtained using an FT-ICR instrument. Magnified regions A, B and C of the main spectrum are presented in the corresponding panels. Labels in panels A-C indicate the length of acyl chain addition to b-AQP0 producing the observed mass, with the arithmetic mean of the peak (modelled as a Gaussian distribution) indicated in parentheses. For the raw LC-MS trace see Fig. S4.

The most abundant species, with an average mass 28225.6, corresponds to an increase by 2.9 Da of the calculated mass of b-AQP0 (28225.7, based on sequence). This increase is accounted for by known deamidations of Asn/Gln residues in AQP0 [5]. Using this species as a reference, a number of modified proteins with increased mass can be identified (Table S1). Included amongst these is a species with a mass increase of 79.9 relative to the major species, corresponding to the known phosphorylation product of bovine AQP0 [14,15]. Human AQP0 (h-AQP0) is similarly phosphorylated [5,13]. Further modifications producing mass increases in the range expected for acyl addition are apparent. These include C16 and C18 (Table S1, entries 2 and 3), for which palmitoyl (C16:0) and oleoyl (C18:1) have previously been described [5], and C20. Higher mass acyl adducts are apparent, corresponding to chain lengths of C22, C26 and C28. The latter two, however, are of very low intensity. It is unclear whether a C24 adduct is present as the expected mass for this adduct is close to that expected for addition of both oleoyl and phosphate groups to b-

AQP0. The latter species is expected to be present based on the observation of its oxidized form (Table S1, entry 8). In addition to these modifications, two further modifications of low abundance can be identified, corresponding to the addition of C36 and C56 (Table S1, entries 11 and 12). Given the high relative abundance of the oleoyl adduct, the most likely assignments for these are  $2 \times \text{C18}$  and  $2 \times \text{C18} + \text{C20}$ . Further species of higher mass (29100–29900 Da) could not be readily identified and are presented in Fig. S5.

#### Analysis of Trypsin Digests

Intact b-AQP0 was subjected to trypsin proteolysis followed by LC-MS analysis of the resulting mixture. Amongst the peptides produced (Fig. S6-S7, Table S2), two sets corresponding to acyl modification at different sites on b-AQP0 were apparent (Fig. 2). For both sets of peptides, the order of elution of the acyl adducts, with retention time increasing with saturated chain length, and decreasing with increasing unsaturation, is in line with experiments on other systems [1,2,16].

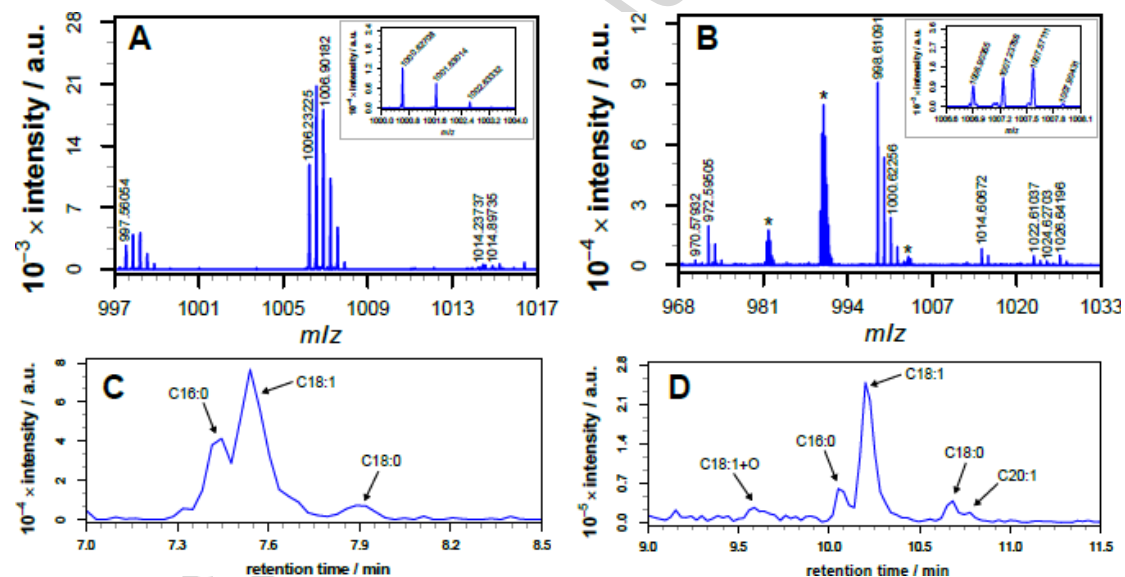


**Figure 2** - Acyl-modified peptides from trypsin digests of b-AQP0 analyzed by LC-MS (FT-ICR). A, summed mass spectrum over the retention time (r.t.) range 7.4–8.0 min. The inset shows the r.t. range 7.85–9.0 min; B, mass spectrum over the r.t. range 9.5–10.9 min. The inset shows the r.t. range 10.6–10.8 min; C, sum of the extracted ion currents (EICs) in the  $m/z$  ranges 997.5–999, 1006–1008 and 1014–1016 (K238 + C16:1–C20:0); D, summed EICs in the  $m/z$  ranges 970.5–971.7, 972.4–975.2, 998.2–1016.8 and 1022.2–1028.7 (N-terminus + C16:1–C20:0). Asterisks indicate non-acylated trypsin digest products. These are filtered out from the EIC in panel D.

The series of peptides that eluted first (Fig. 2A,C, Fig. S9, Table 1) corresponds to acylation of K238 of the protein. At this position, palmitoyl, oleoyl and stearoyl adducts of the 234–259 sequence are clearly resolved. Within this sequence, there is a single internal, highly conserved lysine (K238) [5] that, as expected [2], is not cleaved by trypsin when lipidated. The ion abundances of these acyl adducts are in the order oleoyl > palmitoyl > stearoyl. In addition to these products, ions of low abundance corresponding to C20 adducts could be detected, albeit with high error. Given the weakness of the signals, this high error is unsurprising, but nevertheless the presence of a signal at  $m/z$  1014.23737 ( $z=3$ ) is consistent with the presence of either C20:3 or C20:4.

The second series of peptides, (Fig. 2B,2D, Fig. S8), gives singly charged ions matching residues 1–5 of b-AQP0 corresponding to acylation at the N-terminus. The acyl modifications, in decreasing order of ion abundance (Table 1, Table S3), are: oleoyl (C18:1) >> palmitoyl (C16:0) > stearoyl (C18:0) > eicosenoyl (C20:1) > dihomo- $\gamma$ -linolenoyl (C20:3)  $\approx$  palmitoleoyl (C16:1) > eicosadienoyl (C20:2). The acyl groups found at the N-terminus reassuringly account for many of the species detected in the whole protein spectrum (Fig. 1). Acyl modifications with chain lengths longer than C20 were not detected in trypsin digests because they are much less abundant and therefore likely fall below the detection threshold. An almost identical set of peptides was produced following trypsin digestion of b-AQP0 isolated from the lens nucleus (Fig. S10, Table S4).

**Table 1** - Acylated species formed by trypsin digests of b-AQP0

r.t. / min *	$m/z$ obs †	$m/z$ calc †	Error / ppm	Peak Area / a.u. min‡	Assignment §
7.41	997.56054	997.56018	0.36	163 $\pm$ 38	[234–259] + C16:0
7.54	1006.23225	1006.23207	0.18	602 $\pm$ 81	[234–259] + C18:1
7.57	1014.23737	1014.23207	5.23	6 $\pm$ 5	[234–259] + C20:3
7.60	1014.89735	1014.90395	-6.51	10 $\pm$ 8	[234–259] + C20:2
7.92	1006.90355	1006.90395	-0.39	93 $\pm$ 28	[234–259] + C18:0
9.55	1014.60672	1014.60564	1.07	484 $\pm$ 177	[1–5] + C18:1 + O
9.64	970.57932	970.57942	-0.11	158 $\pm$ 93	[1–5] + C16:1
9.82	1020.60260	1020.59507	7.38	96 $\pm$ 70	[1–5] + C20:4
10.05	972.59505	972.59507	-0.03	1559 $\pm$ 346	[1–5] + C16:0
10.20	1022.61037	1022.61072	-0.34	160 $\pm$ 93	[1–5] + C20:3
10.22	998.61091	998.61072	0.19	6809 $\pm$ 810	[1–5] + C18:1
10.40	1024.62703	1024.62637	0.64	106 $\pm$ 74	[1–5] + C20:2
10.68	1000.62708	1000.62637	0.71	883 $\pm$ 250	[1–5] + C18:0
10.77	1026.64196	1026.64202	-0.06	457 $\pm$ 171	[1–5] + C20:1

\* time of maximum intensity in the EIC

† observed and calculated  $m/z$  values are monoisotopic

‡ errors are reported as the standard error of the mean (n=2)

§ [1–5]: <sup>1</sup>MWELR<sup>5</sup>,  $z=1$ ; [234–259]: <sup>234</sup>LSILKGRPSESNGQPEVTGEPVELK<sup>259</sup>,  $z=3$ ; all [234–259] matches contain one Asn or Gln deamidation

Tandem MS experiments confirmed the lipidation site identities. Targeted fragmentation of oleoyl-modified b-AQP0[1–5] and b-AQP0[234–259] yielded several modified and unmodified *b*- and *y*-ions that were consistent with lipidation of the N-terminus and K238 respectively (Fig. 3A, C, Table S5, S6). LC-MS<sup>E</sup> experiments on the digests (performed on the QToF) yielded profiles with maxima for the intensities of unmodified ions shared by all lipidated peptides at retention times corresponding to the major acyl-modified peptides (Fig. 3B, D). The MS<sup>1</sup> data from these experiments also reproduced the identifications from Table 1. Overall, the high mass accuracy obtained in the FTICR-MS experiments, plus the fragmentation patterns yielded by QToF tandem MS experiments, confirm that these peptides correspond to acyl modifications to the N-terminus and K238 of b-AQP0. The whole protein data (Fig. 1) suggest an additional lipidation site. This site could not be localised from the digest data, either because it was of too low abundance to detect, or because it resulted from lipidation on serine, which is harder to detect [2].

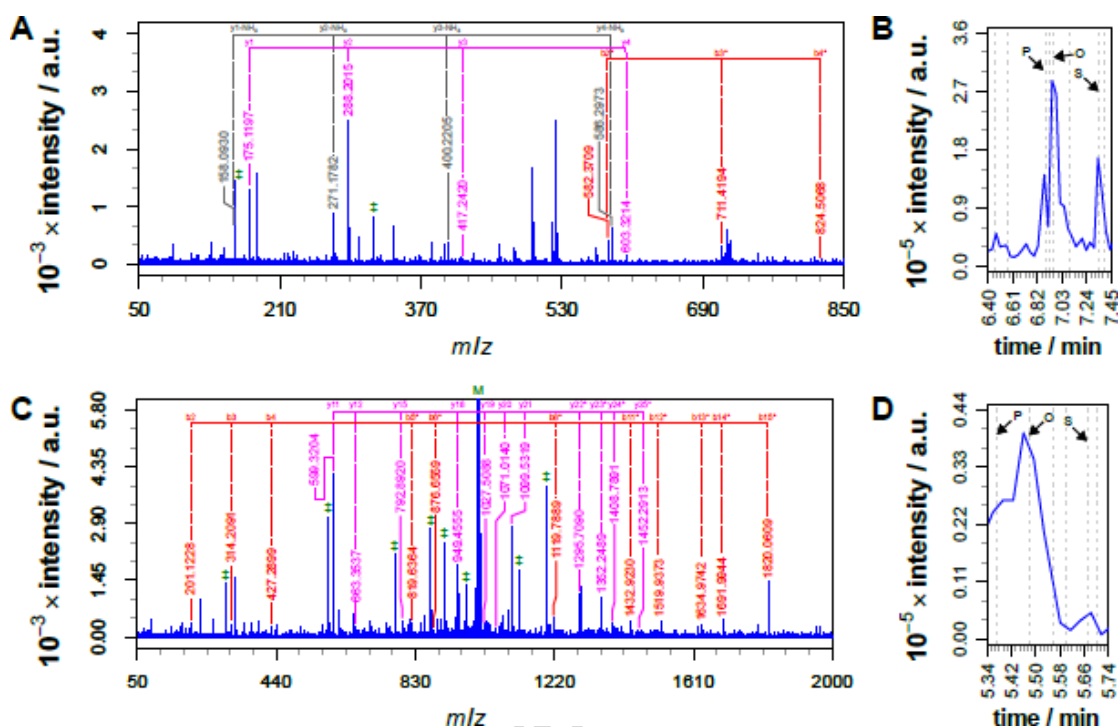


**Figure 3** - LC-MS/MS data for acyl-modified peptides from trypsin digests of b-AQP0. A: MS/MS of oleoyl AQP0[1–5] ( $z=1$ ,  $m/z$  998.61). All  $b$ - and  $y$ -ion ladders are for  $z=1$ ; B: summed extracted ion currents from an  $MS^E$  experiment for the unmodified  $b$ - and  $y$ -ions identified in part A; C: MS/MS of oleoyl AQP0[234–259] ( $z=3$ ,  $m/z$  1006.23). The  $b$ -ion ladder is for  $z=1$  and the  $y$ -ion ladder for  $z=2$ ; D: summed extracted ion currents from an  $MS^E$  experiment for the unmodified  $b$ - and  $y$ -ions identified in part C. In A and C, oleoyl-modified ions are indicated by asterisks; other  $b$ - and  $y$ -ions matching the parent peptide are indicated by double daggers (see Tables S5, S6). In B and D, vertical dashed lines indicate the retention times for acyl modified species, including palmitoyl (P), oleoyl (O) and stearoyl (S).

Similar analyses were conducted for h-AQP0 isolated from the outer cortex of the human lens (Fig. S11, Table S7). The N-terminal residues of h-AQP0 and b-AQP0 are identical, resulting in similar lipidated peptides (Fig. S12, Table S8), with the following acyl modifications found in decreasing order of abundance: oleoyl  $\gg$  palmitoyl  $>$  stearoyl  $>$  arachidonoyl  $\approx$  palmitoleoyl  $>$  eicosenoyl. In addition to these species, oxidized counterparts resulting from the addition of between one and three oxygens were abundant. Indeed, dihomo- $\gamma$ -linolenoyl (C20:3) modifications were only detected in the oxidized form. Such oxidations were anticipated, as methionine and tryptophan oxidations have been documented previously for h-AQP0 [5,13]. For both the arachidonoyl and dihomo- $\gamma$ -linolenoyl adducts, however, two different oxidized products were detected, a pattern not repeated with other acyl groups. This suggests that oxidation occurs at sites within the chain when the acyl group is polyunsaturated. Analysis of the lipidation profile of h-AQP0 peptides containing K238 was more challenging due to the presence of significant levels of other modifications, including phosphorylation, deamidation, oxidation and truncation (at residues 243, 246 and 259) [5,13,15]. Spectral complexity increased, with more instances of spectral overlap, decreasing the ion count for each lipidated species. Peptides in the 229–263 sequence of h-AQP0, spanning K238, were lipidated with oleoyl, palmitoyl and arachidonoyl groups (Fig. S13-S14, Table S9). A stearoyl-modified product was also present, although this peptide was not completely resolved

chromatographically from its oleoyl-modified counterpart. In addition, two oxidized peptides with highly unsaturated acyl chains, C22:5 and C20:5, were tentatively identified. Lipidated versions of truncated sequences were present, indicating that truncation and lipidation are not mutually exclusive events.

#### 4. Discussion

A key prediction concerning non-enzymatic acyl transfer from membrane lipids to a target protein is that the lipidation profile will resemble the fatty acid profile of the membrane leaflet proximal to the target site. The two potential acylation sites in AQP0, the N-terminus and K238, are both adjacent to the cytoplasmic leaflet of lens cortex plasma membranes based on the available crystallographic data [17] and therefore their lipidation profiles would be expected to match that profile. Our own calculations predict that the 214–263 sequence of h-AQP0 forms a lipid-binding amphipathic helix (Fig. S15, Table S10). K238 lies at the boundary between polar and non-polar surfaces of the helix, a feature that is known to promote acyl transfer from lipids to peptides that localize interfacially [1].

The asymmetry of lens membranes is not well characterized, but it is expected that the younger cells in the outer part of the cortex retain the leaflet asymmetry typical of most mammalian plasma membranes, with phosphatidylethanolamine (PE), phosphatidylserine (PS) and phosphatidylinositol (PI) lipids enriched in the cytoplasmic leaflet and phosphatidylcholine (PC) and sphingolipids such as sphingomyelin (SM) enriched in the exoplasmic leaflet [18,19]. As a consequence, acyl transfer from the membrane to AQP0 would be expected produce a distribution of acyl groups that reflects the acyl composition of PE and PS, and to a lesser extent (due to their low abundance), PI lipids.

The major lipid classes of bovine lens membranes are, in decreasing order of abundance, PC  $\approx$  PE  $\approx$  SM  $>$  PS  $>$  PI (when PE plasmalogens are included in the PE fraction) [20,21]. Cholesterol is also a major component [22,23]. As a whole, the abundance of the major fatty acid constituents of bovine lens lipids decreases in the order C16:0  $>$  C18:1  $>$  C24:1  $>$  C18:0  $>$  others [24]. Of the others, C14:0, C16:1, C20:0–4, C22:0–2, and C24:0 have been described [25,26]. Small quantities of other potential acyl donors are present, including PE plasmalogens, and *lyso*-lipids (*lyso*-PC and *lyso*-PE) [24]. All of the C24:1 (nervonoyl) fatty acyl groups are associated with SM in the form of an amide and therefore will not undergo uncatalysed acyl transfer reactions with proteins. A closer inspection reveals that C18:1 (oleoyl) is the major acyl group associated with PE and PS, whereas C16:0 (palmitoyl) is mostly associated with PC. Specifically, the acyl composition in weight% for bovine lens PE lipids decreases in the order C18:1 (63.8)  $\gg$  C16:0 (12.9)  $>$  C18:0 (9.5)  $>$  C16:1 (3.3)  $>$  C22:0 + C22:3 (2.9)  $>$  C20:1 (1.9) [24]. Similar trends are found by MS-based lipidomics [27]. PS lipids have a fatty acyl composition that is broadly similar to that of PE.

Human lens membranes are significantly more enriched in cholesterol and sphingolipids than bovine lens membranes [20,21]. Within the sphingolipids, there is a pronounced shift to longer and more saturated alkyl chains [27], which is reflected in the fatty acid distribution for the membrane as a whole [28]. In contrast to bovine lens membranes, however, the predominant glycerophospholipid class is PE, with the abundance of lipid classes being PE  $>$  PC  $>$  PS  $\gg$  PI. In the PE and PS lipid classes, ether and vinyl ether linked plasmalogens represent the major lipid types [27]. The

content of ester-linked fatty acyl groups within the PE lipids, i.e. those that are “transferrable” by aminolysis, decreases in the order C18:1 >> C20:4 > C18:0 > C16:0 > C22:3 ≈ C22:4 > C22:6 ≈ C22:5 ~ C16:1. In the PS lipids, the trend is broadly similar: C18:1 >> C18:0 > C20:4 ≈ C16:0 > C22:6 ≈ C20:1. It is notable that we have detected h-AQP0 modifications with the majority of these fatty acyl groups, including some, such as C22:5, that are absent from b-AQP0. This species difference can be considered also as evidence for non-enzymatic lipidation.

If lipidation occurs from the membrane, the abundance of each acyl modification of AQP0 should correlate with the amount of that acyl group that is transferrable from host membranes. The quality of this correlation is striking for each family of acyl modified peptides from AQP0 ([234-259] for b-AQP0, [229-263] for h-AQP0, [1-5] for both) when the fatty acyl composition of the major PE component of lens cortex is considered (Fig. 4). Bovine AQP0 in particular produces extremely strong correlations for both lipidation sites. These correlations are equally good when a different dataset is used for the PE acyl composition (Fig. S16, Table S11).

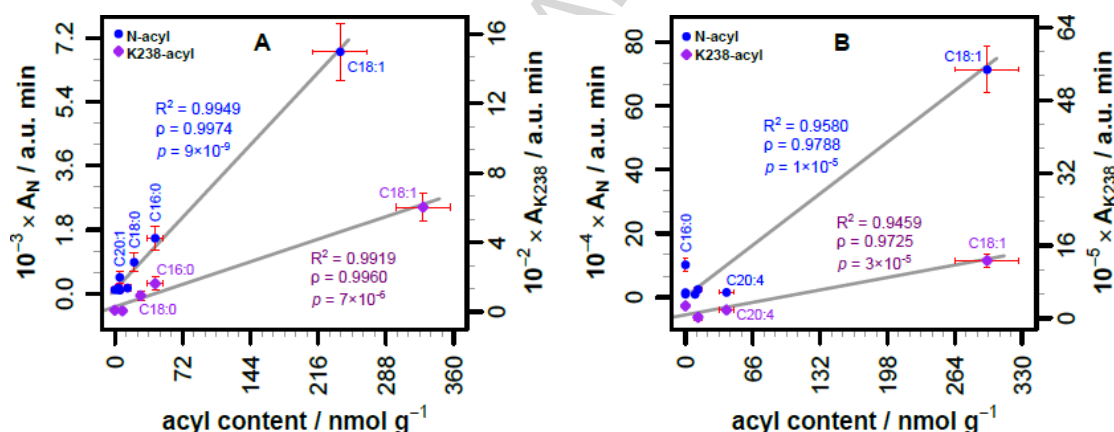


**Figure 4** - Correlations (shown as points) between the peak areas of lipidated peptides from b-AQP0 (A) and h-AQP0 (B), modified at the N-terminus (circles) and K238 (diamonds), and the transferrable (ester-linked) fatty acyl content of lens PE (PE in A, PE plasmalogen in B). Peak areas ( $A_N$  and  $A_{K238}$  for N-terminal and K238 modifications respectively) were calculated from the EIC of each species, using the monoisotopic ion in A and the full isotopomer envelope in B. The acyl content was calculated using the data of Deeley *et al* [27] (Table S12-S13). Error bars are  $2 \times$  SEM ( $n=4$  for acyl content,  $n=2$  and  $4$  for peak areas in A and B respectively). The line and the  $R^2$  statistic are from linear regression analysis. The  $p$ -value is the Pearson correlation coefficient and the  $p$ -value a t-test of the correlation coefficient.

Both lipidation sites produce better correlations for b-AQP0 than h-AQP0 due to the complexity of the additional posttranslational modifications seen with h-AQP0. Oxidative damage to polyunsaturated acyl groups (discussed above) will reduce the peak intensities of peptides modified with these acyl groups and will mean their abundance is under-represented. It is also apparent when considering Fig. 4B that for PE lipids, oleoyl (C18:1) is an order of magnitude more abundant than any other acyl group in both the lipidation and the lipid content data. This high oleoyl abundance reflects a very skewed spread of acyl content values. The correlation in Fig. 4B is therefore very sensitive to the magnitude of the oleoyl peak and the underlying correlation of the other points is much weaker when C18:1 is omitted. This is not the

case for the bovine data, for which strong correlations exist even when the C18:1 point is not included (Fig. S17). The data point for C16:0 in Fig. 4B is notably different from the others, with a much higher prevalence in lipidated h-AQP0 than lens PE. As the transferrable C16:0 content of human lens PC is significantly higher, it may be that a mixed model of transfer from both PE and PC is more appropriate. Analysis of b-AQP0 from the lens nucleus revealed higher levels of N-terminal lipidation (compared to cortex b-AQP0) and similar levels of K238 lipidation, with good correlations between lipidation profile and PE composition (Fig. S18). This increase in lipidation levels in the post-mitotic cells of the lens nucleus, whilst a strong positive correlation with PE fatty acyl composition is retained, is additional evidence for non-enzymatic lipidation. Fig. 4 presents the best overall correlations for both proteins. Good correlations are produced for both proteins with other PE and PS components, but much poorer correlations are produced with PC and total fatty acid compositions (Fig. S19-S21).

For AQP4, enzymatic palmitoylation was suggested to have a functional role in preventing the formation of square arrays [29]. We note that the sites for AQP0 lipidation (M1 and K238) are adjacent to major N- and C-terminal truncation sites (2 and 239) [30] in human AQP0. It has been suggested that lipidation might encourage the partitioning into ordered (detergent resistant) domains of the membrane [5], but we suggest the regulation of post-translational modifications and protein-protein interactions could also be feasible functional consequences of this non-enzymatic lipidation. It is notable also that K238 is highly conserved.

Given the range of acyl modifications to AQP0 that we have found, alongside the moderate overall extent of modification, enzymatic lipidation of AQP0 would require an enzyme that exhibits both poor acyl group selectivity (but nevertheless favours oleoyl transfer) and low efficiency. Such an enzyme has not been described. It seems more probable that lipidation occurs *via* acyl group transfer from membrane lipids, as this method accounts both for the low efficiency of transfer and the differences we observed between human and bovine lipidation profiles. Here we have provided evidence that acyl group diversity at the modification sites of AQP0 closely matches that of PE lipids, which are a major constituent of the membrane leaflet proximal to both the N- and C-terminal AQP0 lipidation sites.

### Acknowledgements

The authors thank the Ministry of Higher Education and Scientific Research of the Kurdistan Regional Government for funding (VSI). The financial support of Fight for Sight UK and the Leverhulme Trust (RAQ) is gratefully acknowledged.

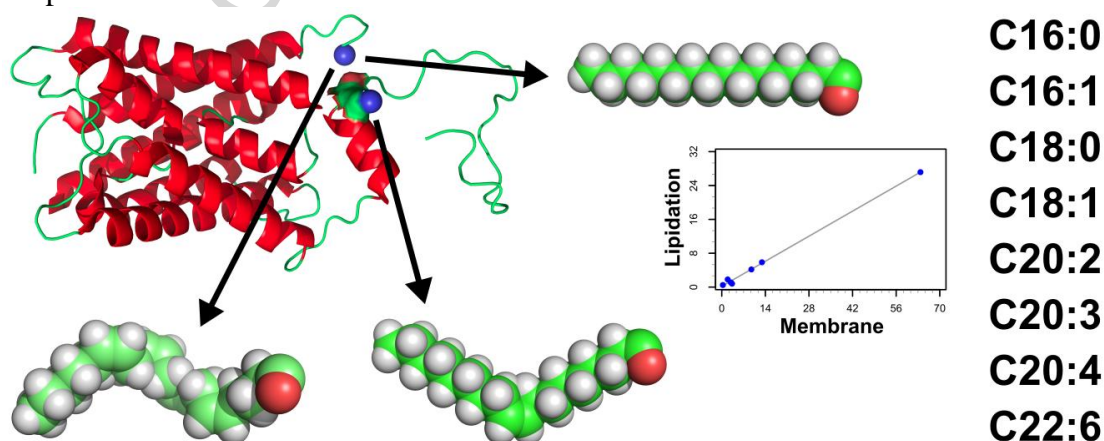
### References

- [1] R. H. Dods, B. Bechinger, J. A. Mosely, J. M. Sanderson, Acyl transfer from membrane lipids to peptides is a generic process, *J. Mol. Biol.* 425 (2013) 4379–4387. (10.1016/j.jmb.2013.07.013)
- [2] R. H. Dods, J. A. Mosely, J. M. Sanderson, The innate reactivity of a membrane associated peptide towards lipids: acyl transfer to melittin without enzyme catalysis, *Org. Biomol. Chem.* 10 (2012) 5371–5378. (10.1039/c2ob07113d)
- [3] C. J. Pridmore, J. A. Mosely, A. Rodger, J. M. Sanderson, Acyl transfer from phosphocholine lipids to melittin, *Chem. Commun.* 47 (2011) 1422–1424.

- (10.1039/C0CC04677A)
- [4] A. Hentschel, R. P. Zahedi, R. Ahrends, Protein lipid modifications-More than just a greasy ballast, *Proteomics* 16 (2016) 759–782. (10.1002/pmic.201500353)
- [5] K. L. Schey, D. B. Gutierrez, Z. Wang, J. Wei, A. C. Grey, Novel fatty acid acylation of lens integral membrane protein aquaporin-0, *Biochemistry* 49 (2010) 9858–9865. (10.1021/bi101415w)
- [6] J. Han, K. L. Schey, Proteolysis and mass spectrometric analysis of an integral membrane: aquaporin 0, *J. Proteome Res.* 3 (2004) 807–812. (10.1021/pr049945w)
- [7] J. L. Wenke, K. L. Rose, J. M. Spraggins, K. L. Schey, MALDI Imaging Mass Spectrometry Spatially Maps Age-Related Deamidation and Truncation of Human Lens Aquaporin-0, *Invest. Ophthalmol. Vis. Sci.* 56 (2015) 7398–7405. (10.1167/iovs.15-18117)
- [8] S. Manenti, I. Dunia, E. L. Benedetti, Fatty acid acylation of lens fiber plasma membrane proteins. MP26 and alpha-crystallin are palmitoylated, *FEBS Lett.* 262 (1990) 356–358. (10.1016/0014-5793(90)80228-B)
- [9] S. Bassnett, Y. Shi, G. F. Vrensen, Biological glass: structural determinants of eye lens transparency, *Philos. Trans. R. Soc. Lond. B Biol. Sci.* 366 (2011) 1250–1264. (10.1098/rstb.2010.0302)
- [10] J. Johansson, Structure and properties of surfactant protein C, *Biochim. Biophys. Acta* 1408 (1998) 161–172. (10.1016/S0925-4439(98)00065-9)
- [11] L. C. Milks, N. M. Kumar, R. Houghten, N. Unwin, N. B. Gilula, Topology of the 32-kd liver gap junction protein determined by site-directed antibody localizations, *EMBO J.* 7 (1988) 2967–2975.
- [12] M. D. Perng, A. Sandilands, J. Kuszak, R. Dahm, A. Wegener, A. R. Prescott, R. A. Quinlan, The intermediate filament systems in the eye lens, *Methods Cell Biol.* 78 (2004) 597–624. (10.1016/S0091-679X(04)78021-8)
- [13] K. L. Schey, A. C. Grey, J. J. Nicklay, Mass spectrometry of membrane proteins: a focus on aquaporins, *Biochemistry* 52 (2013) 3807–3817. (10.1021/bi301604j)
- [14] P. D. Lampe, R. G. Johnson, Amino acid sequence of in vivo phosphorylation sites in the main intrinsic protein (MIP) of lens membranes, *Eur. J. Biochem.* 194 (1990) 541–547. (10.1111/j.1432-1033.1990.tb15650.x)
- [15] K. L. Schey, J. G. Fowler, J. C. Schwartz, M. Busman, J. Dillon, R. K. Crouch, Complete map and identification of the phosphorylation site of bovine lens major intrinsic protein, *Invest. Ophthalmol. Vis. Sci.* 38 (1997) 2508–2515.
- [16] M. I. Avelano, M. VanRollins, L. A. Horrocks, Separation and quantitation of free fatty acids and fatty acid methyl esters by reverse phase high pressure liquid chromatography, *J. Lipid Res.* 24 (1983) 83–93.
- [17] T. Gonen, Y. Cheng, P. Sliz, Y. Hiroaki, Y. Fujiyoshi, S. C. Harrison, T. Walz, Lipid-protein interactions in double-layered two-dimensional AQP0 crystals, *Nature* 438 (2005) 633–638. (10.1038/nature04321)
- [18] G. van Meer, D. R. Voelker, G. W. Feigenson, Membrane lipids: where they are and how they behave, *Nature Reviews Molecular Cell Biology* 9 (2008) 112–124. (10.1038/nrm2330)
- [19] P. Devaux, A. Herrmann, Transmembrane Dynamics of Lipids, In: *Wiley Series in Protein and Peptide Science* (V. N. Uversky, Series Ed.), John Wiley & Sons, Hoboken, New Jersey, 2012. (10.1002/9781118120118)
- [20] D. Borchman, M. C. Yappert, M. Afzal, Lens lipids and maximum lifespan, *Exp. Eye Res.* 79 (2004) 761–768. (10.1016/j.exer.2004.04.004)

- [21] D. Borchman, M. C. Yappert, Lipids and the ocular lens, *J. Lipid Res.* 51 (2010) 2473–2488. (10.1194/jlr.R004119)
- [22] C. R. Fleschner, R. J. Cenedella, Lipid composition of lens plasma membrane fractions enriched in fiber junctions, *J. Lipid Res.* 32 (1991) 45–53.
- [23] P. S. Zelenka, Lens lipids, *Curr. Eye Res.* 3 (1984) 1337–1359. (10.3109/02713688409007421)
- [24] R. E. Anderson, M. B. Maude, G. L. Feldman, Lipids of ocular tissues. I. The phospholipids of mature rabbit and bovine lens, *Biochim. Biophys. Acta* 187 (1969) 345–353. (10.1016/0005-2760(69)90008-3)
- [25] H. Hatcher, J. S. Andrews, Changes in lens fatty acid composition during galactose cataract formation, *Investigative Ophthalmology* 9 (1970) 801–806.
- [26] R. M. Broekhuysse, W. J. Soeting, Lipids in tissues of the eye. XV. Essential fatty acids in lens lipids, *Exp. Eye Res.* 22 (1976) 653–657. (10.1016/0014-4835(76)90010-5)
- [27] J. M. Deeley, T. W. Mitchell, X. Wei, J. Korth, J. R. Nealon, S. J. Blanksby, R. J. W. Truscott, Human lens lipids differ markedly from those of commonly used experimental animals, *Biochim. Biophys. Acta* 1781 (2008) 288–298. (10.1016/j.bbalip.2008.04.002)
- [28] G. L. Feldman, T. W. Culp, L. S. Feldman, C. K. Grantham, H. T. Jonsson, Phospholipids of the Bovine, Rabbit, and Human Lens, *Invest. Ophthalmol.* 3 (1964) 194–197.
- [29] H. Suzuki, K. Nishikawa, Y. Hiroaki, Y. Fujiyoshi, Formation of aquaporin-4 arrays is inhibited by palmitoylation of N-terminal cysteine residues, *Biochim. Biophys. Acta* 1778 (2008) 1181–1189. (10.1016/j.bbamem.2007.12.007)
- [30] A. Korlimbinis, Y. Berry, D. Thibault, K. L. Schey, R. J. W. Truscott, Protein aging: truncation of aquaporin 0 in human lens regions is a continuous age-dependent process, *Exp. Eye Res.* 88 (2009) 966–973. (10.1016/j.exer.2008.12.008)

## Graphical Abstract



## Highlights

- Human and bovine aquaporin-0 are lipidated at the N-terminus and K238.
- At each site, an array of acyl groups is found.
- Acyl groups include C16:0, C16:1, C18:0, C18:1, C20:1, C20:2, C20:3, C20:4.

- Acyl group abundance correlates with the acyl content of lens PE lipids.

ACCEPTED MANUSCRIPT